Towards AquaSun practical utilization: Strong adhesion and lack of ecotoxicity of solar-driven antifouling sol-gel coating

Antonino Scurria [a], Cristina Scolaro [b], Silvia Sfameni [a,b], Gabriella Di Carlo [c], Mario Pagliaro [a], Annamaria Visco [b,d,**], Rosaria Ciriminna [a,*]

[a] *Istituto per lo Studio dei Materiali Nanostrutturati, CNR, via U. La Malfa 153, 90146 Palermo, Italy*
[b] *Dipartimento di Ingegneria, Università di Messina, Contrada di Dio, Villaggio S. Agata, 98166 Messina, Italy*
[c] *Istituto per lo Studio dei Materiali Nanostrutturati, CNR, via Salaria km 29.3, 00015 Monterotondo, RM, Italy*
[d] *Istituto per i Polimeri, Compositi e Biomateriali, CNR, via P. Gaifami 18, 95126 Catania, Italy*

ARTICLE INFO

ABSTRACT

The outcomes of adhesion and ecotoxicity tests carried out on metal specimens faithfully representing the surface of real ships, including the primer and tie coat layers typically applied on ship hull prior to deposition of the antifouling paint, show the practical applicability of "AquaSun" antifouling sol-gel coatings. Newly developed AquaSun coatings share hydrophobicity (contact angle >115°) and exceptionally high scratch resistance (ASTM 5B). Coupled to the ecofriendly antifouling mechanism based on continuous H_2O_2 formation upon exposure to solar light and foul release due to low surface energy, these results open the route to the practical utilization of these novel marine coatings.

1. Introduction

Protection of ships and boats from marine and lake biofouling applying on the hull an antifouling (AF) paint is an unavoidable necessity. A ship without protection after 6 months will consume 40% more "bunker" fuel oil (and engine power output) due to additional dragging and friction originating from the surface roughness of macro- and microorganisms foulant organisms accumulating on the unprotected hull [1]. Following the global ban of highly toxic tributyltin-based paints, the most commonly used AF coatings today are based on the biocidal action of copper oxide (Cu_2O) and copper thiocyanate (CuSCN) typically formulated at 20–40% concentrations in combination with "booster" biocides, such as copper or zinc pyrithione, and other synthetic antifungal, herbicide, and pesticide synthetic molecules originating from crop protection research in agriculture [2]. The amount of AF paints globally consumed by the world's fleet grows at 10% annual rate [3]. Hence, the >80,000 t annual consumption estimated by an industry's practitioner in 2010 [4], now largely exceeds the 100,000 t threshold. One such paint is designed to last 3–5 years, gradually releasing all the incorporated biocides, causing a significant (and global) impact on marine life [5].

For example, a recent study on copper-based paints in the Venice lagoon revealed that copper leached by these paints has potential disruptive effects on the biodiversity of coastal macrofouling communities affecting both the settlement and growth of key species of macrofouling of hard-substrata [6].

Based either on less toxic biocides, or on foul-release (FR) polymeric coatings, in the last two decades (2000−2020) new environmentally benign antifouling paints have been commercialized [7,8]. Amid them, the waterborne xerogel thin coatings made of organically modified silica (ORMOSIL) developed by Detty and Bright in the early 2000s [9], were first commercialized (with the AquaFast tradename) in the early 2010s [10]. Their efficacy relies on the FR activity imparted to the hull by the thin hydrophobic ORMOSIL layer [11]. Biofoulants sticking loosely to the hull are released even at low cruising speed. Unfortunately, these ecofriendly, biocide-free coatings do not exert antifouling action when the vessel stands still, for example in port waters.

Named AquaSun, an ORMOSIL-based coating showing excellent AF activity due to solar-driven photocatalytic generation of H_2O_2 and hydroxyl radicals, is comprised of thin film (3 μm thick) of methylated silica sol-gel derived from a sol containing 50 mol% methyltriethoxysilane (MTES) and 50 mol% of tetraethyl orthosilicate

(TEOS) encapsulating flower-like microparticles of the visible-light photocatalyst Bi_2WO_6 [12]. As shown by investigation of the anti-fouling effect of hydrogen peroxide release from enzymatic marine coatings [13], H_2O_2 degrades the adsorbed species forming hydroxyl radicals (HO•) [14].

Tested under real life situations irradiating with (simulated) solar light for over 3 months a substrate coated with AquaSun immersed in the waters of Indian Ocean, the coating retained its excellent original AF activity [15]. Remarkably, indicating no saturation effects, the activity degradation rate was found to be linear with about half of 1 ppm of added uracil being degraded in three days [12]. Under solar light, marine phytoplankton microorganisms consuming inorganic carbon give place to photosynthesis providing organic matter for the organisms that comprise the majority of marine life [16]. The same coating also shares good FR properties, as shown by full release in water in 2 h only of all the adenine adsorbed from a 1 ppm solution, even in the absence of light irradiation. Given the high stability, low cost, and environmentally benign nature of silica-based sol-gel coatings, the study concluded that "the technology has significant potential toward replacing conventional antifouling and foul-release coatings with a single product of broad applicability" [15]. On path to demonstrate the practical applicability of this new marine AF/FR coating, now we report the outcomes of adhesion experiments on real ship steel substrates as well as the first ecotoxicity experiments.

2. Experimental methods

2.1. Preparation of the xerogel films and topcoat deposition

All chemicals were purchased by Sigma-Aldrich (now Merck, Milano, Italy) and used as such, without further purification. C18 stands for *n*-octadecyltrimethoxysilane. C8 stands for *n*-octyltriethoxysilane. The AquaSun xerogel film was prepared starting from a formulation incorporating 12% w/w of Bi_2WO_6 (with respect to the theoretical weight of silica) suspended in the C18 1%/C8 49%/TEOS 50% silicon alkoxide solution in 2-propanol through hydrolytic polycondensation under acidic conditions (HCl 0.1 N). In detail, a 10 mL flask was added under vigorous stirring with TEOS (4 mmol, 0.89 mL), C8 (3.92 mmol, 1.30 mL), C18 (0.08 mmol, 40 µL), 2-propanol (2.6 mL) and HCl 0.1 M (0.5 mL). The resulting solution was left under stirring for 24 h after which an aliquot of Bi_2WO_6 (55.8 mg, 12% w/w) was added under stirring. The resulting xerogel film was named THA8. A blank film devoid of bismuth wolframate was also prepared and named THA8B. These coatings were deposited on pre-treated real ship steel substrates by simple coating the pre-treated surface with a brush. In detail, the metal plate was pretreated with the tie coat paint (Jotun, Sandefjord, Norway). The latter paint was prepared by mixing three different components: component A (40 g, Safeguard Universal ES Comp A), component B (8 g, Safeguard Universal ES Comp B) and finally the solvent (5 g, Jotun Thinner No. 17). The tie coat was deposited using a roll while THA8 and THA8B were deposited with a paintbrush. The aforementioned and related sol-gel coatings functionalized with Bi_2WO_6 were coated on glassy substrates for scanning electron microscopy investigation. Prior to deposition of the xerogel film *via* spin coating each glass was cleaned by leaving it in contact with a concentrated (1 M) HCl aqueous solution for 24 h, followed by extensive washing with triple distilled water and ethanol and drying in open air.

2.2. SEM imaging and energy-dispersive spectroscopy

The coating surface investigation and dopant particle morphology were analyzed a high brilliance Zeiss LEO 1530 field emission scanning electron microscope (FE-SEM; Carl Zeiss, Oberkochen, Germany) apparatus equipped with an energy dispersive X-ray spectrometer (EDS) INCA 450 (Oxford Instruments, Abingdon, Great Britain) and a four sector back-scattered electron (BSE) and secondary electron (SE)

detectors. FE-SEM investigations were performed by using both SE and BSE electrons and selecting an acceleration voltage of 20 kV.

2.3. Surface roughness, contact angle, adhesion test, thickness measurement and viscosity experiments

The surface roughness (R_a) of the xerogel films was measured with a Surftest SJ-210 - Series 178 surface roughness tester (Mitutoyo, Milan, Italy) using Eq. (1), in which R_a is calculated as the arithmetic mean of the absolute values of the deviations of the evaluation profile (Yi) from the mean line.:

$$R_a = \frac{1}{N} \sum_{i=1}^{n} |Yi| \tag{1}$$

The contact angle θ was assessed by the sessile drop method by means of a prototype instrument at the Engineering Department of Messina University, which measures the contact angle of 1 µL drop of deionized water of on the horizontal surface of the film. The wet ability was derived from Eqs. (2) and (3):

$$\theta_w = 2 arctg \left(\frac{2h}{d} \right) \tag{2}$$

$$\theta_Y = arcos \left(\frac{cos\theta_w}{r} \right) \tag{3}$$

where d is the diameter and h the height (both in mm) of the drop, θ_w is the Wenzel angle apparent dependent on the roughness of the surface, r is the surface roughness (R_a), and θ_Y is the Young contact angle of equilibrium on a perfectly smooth surface.

The adhesion of coating films to metallic substrate was evaluated by cross-cut test using a commercial Cross Hatch Adhesion Tester (SAMA Tools SADT502-5, SAMA Italia, Viareggio, Italy) according to ASTM D3359e2 Standard Test Method for Measuring Adhesion by Tape Test. Using an appropriate cutter, a grid incision was made in a test area of approximately 10×10 cm, creating a grid of horizontally and vertically spaced (2 mm) incisions across the surface. All the particles produced in the area were then removed with a soft brush. As a rule, a 3 M adhesive tape is stuck onto the cutting grid with a finger, applying a light pressure. It is subsequently removed with an even peeling movement. The test is evaluated visually by comparing the sectional grid image with the reference images from ISO 2409:2013. Depending on the condition of the damage, a cross-cut parameter from 0 (very good adhesive strength) to 5 (very poor adhesive strength) is assigned according to the number of squares that have flaked off and the appearance.

To measure the thickness of coatings on metal bases in a non-destructive way, a digital thickness gauge for high precision coating thickness measurements (SAMA Tools SA8850, SAMA Italia, Viareggio, Italy) was used. A map was drawn on each rectangular 150 mm × 75 mm, 5 mm thickness steel specimen, covered with the antifouling coating, which identifies a grid of 84 (14×6) points. At each point of the resulting grid, thickness measurements were made by placing the probe perpendicular to the specimen. The mean values of all measurements were then calculated.

The flow behavior of liquid-like samples at room temperature was analyzed through a rotational rheometer (MC-502, Anton Paar, Graz, Austria) consisting of a rotating rod immersed in the liquid to be analyzed. The terminal part of the rod has a specific shape (geometry). Measurements for this work were carried out by using the cone-plate geometry. For each geometry the lower support was always fixed (only the upper part is connected to the motor moves). Each viscosity test was performed at room temperature of 25 °C within the shear rate from $0.01\ s^{-1}$ up to $1000\ s^{-1}$. Each test was carried out three times. The linear viscoelasticity region (LVR) was checked by an amplitude sweep test of both the topcoats THA8 and THA8B at a constant frequency of 1 Hz.
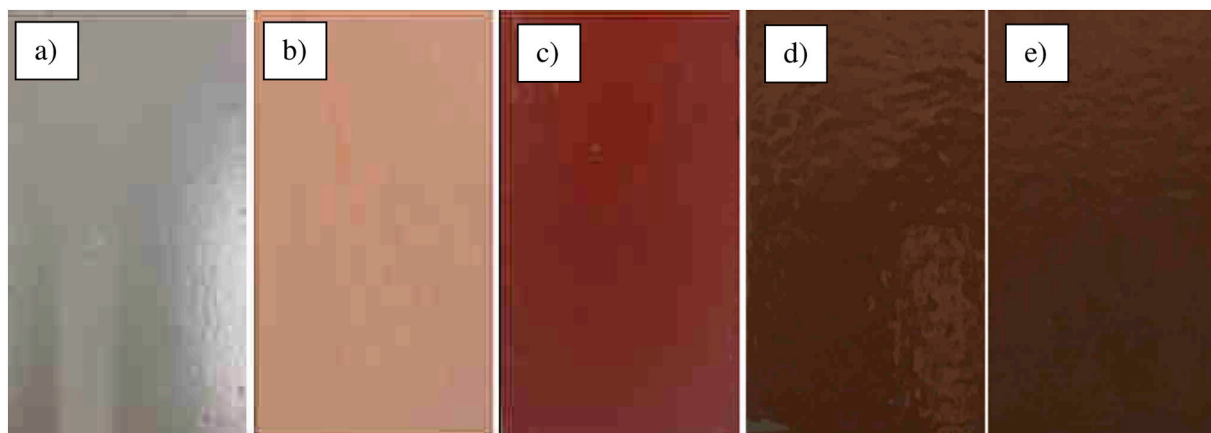
Fig. 1. Metal plate gray color before (a) and after the progressive addition of: pink-color primer (b), red-color tie coat (c), brown-color topcoat THA8 (d), and topcoat THA8B (e). (For interpretation of the references to color in this figure legend, the reader is referred to the web version of this article.)

2.4. Microtox test

The Microtox toxicity tests were carried out according to the standard procedures described in EN12457, using standardized (ISO) seawater at 100 mg/L starting concentration.

2.5. Statistical analysis

Prism 8.0.2 statistical software (GraphPad, Inc., La Jolla, CA, USA) was used for the statistical analysis. Data are reported as mean ± SD (±Standard Deviation) at a significance level of $p < 0.05$. The D'Agostino & Pearson test was used for normality test of data, and Brown-Forsythe test for homogeneity of the variance test. Since all data used in this study satisfied these two tests, one-way analysis of variance (ANOVA) with Tukey's post-hoc test was performed to evaluate the statistical significance of the differences between the groups (significance level: 0.05).

3. Results and discussion

In 2011, Detty, Bright and co-workers reported that the original AquaFast formulation (1:1 C8/TEOS) could be substantially improved with respect to the foul release of juvenile barnacles and sporeling biomass by simply adding a 1% (in molar terms) of C18 (*n*-octadecyl-trimethoxysilane) to the sol-gel formulation [17]. Expanding on these previous findings we prepared an AquaSun xerogel film starting from the same formulation incorporating Bi_2WO_6 suspended in the pre-hydrolyzed C18/C8/TEOS Si alkoxide solution in aqueous propanol. The resulting xerogel film was named THA8B. A blank film devoid of bismuth wolframate (THA8) was also prepared. The images in Fig. 1a–e, show real ship steel substrates pre-treated with primer and tie coat further coated with a thin layer of these sol-gel coatings deposited by simple brushing with a paintbrush. The chromatic variation indicates the deposition steps of the various layers of paint. In particular, the typical gray color of steel turns pink once the first primer layer has been deposited, then red after the second tie-coat layer is deposited, and
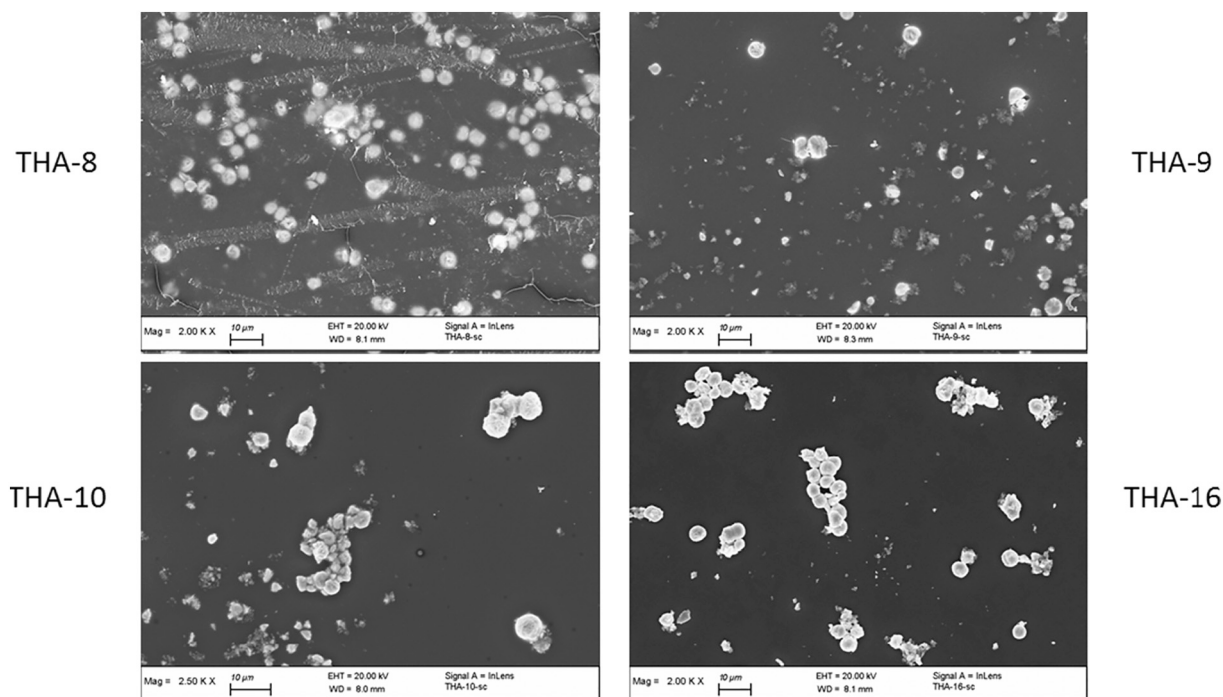

Fig. 2. FE-SEM photographs of different AquaSun xerogel films deposited on glass (for xerogel composition, see Table 3).
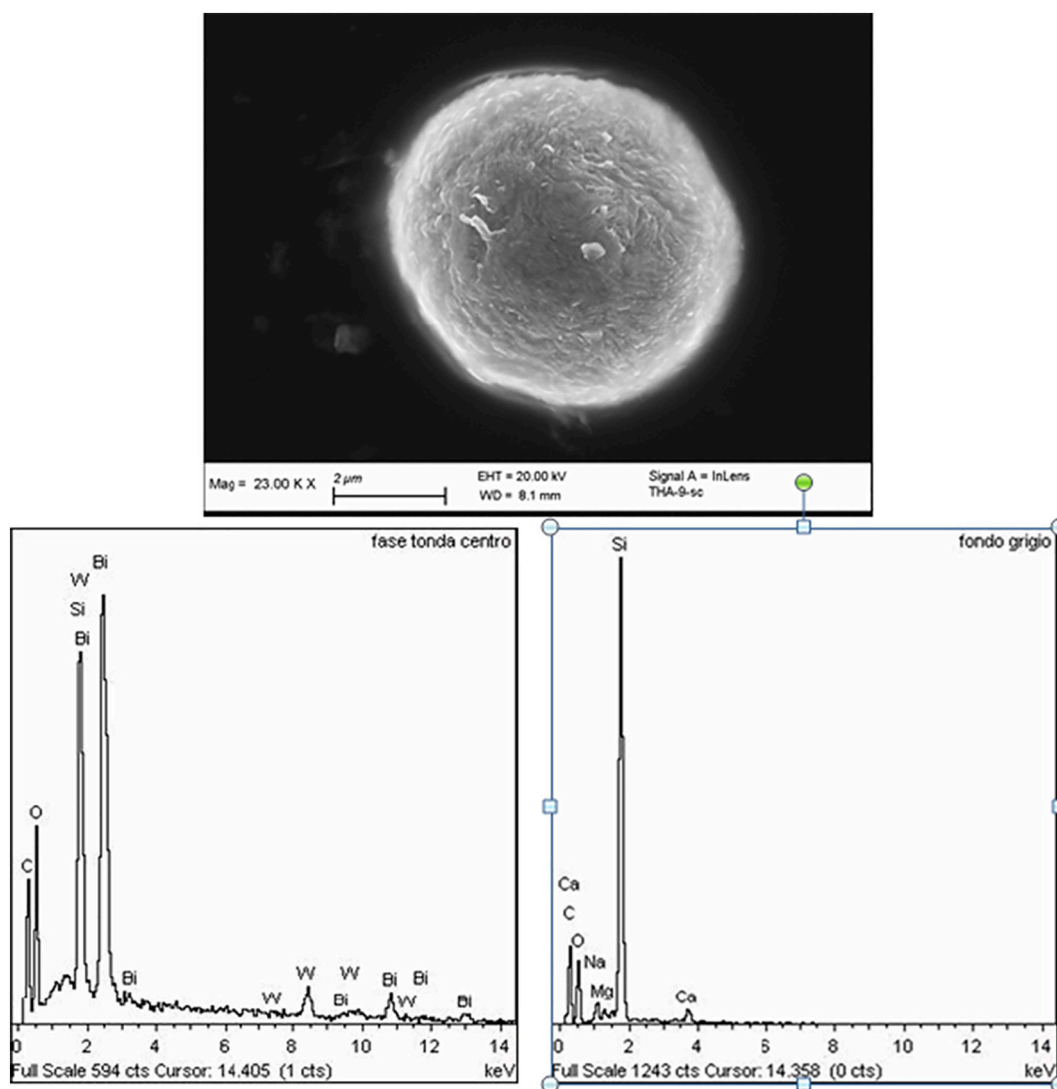
Fig. 3. FSE-SEM image of a flower-like Bi_2WO_6 microparticle encapsulated in the THA-9 sc AquaSun xerogel (for xerogel composition, see Table 3) deposited on glass (top). EDS spectra of the encapsulated microparticle (bottom left) and embedding organosilica matrix (bottom right).

finally brown upon deposition of the third and last layer of antifouling topcoat. Both primer and tie coat make the surface opaque due to the rough consistency of both coatings. On the other hand, after the deposition of both AquaSun topcoats (THA8 and THA8B), the material appears shiny due to the glassy nature of the ORMOSIL coating. The smooth surface of the last layer suggests the possibility of a lower wettability of the topcoat compared to both the primer and the tie coat.

The ability of ORMOSIL sol-gel coatings to modify the contact angle and the roughness of the coated surface was proven in a broad interval of ORMOSIL xerogel film compositions, using three different alkyl-modified Si alkoxides of different alkyl length (C1, C3, and C18; for the xerogel composition, see Table 3). Fig. 1 further shows the metal substrate with the tie coat only, and the same substrate following application of THA8. Clearly the coating is homogeneously deposited. The SEM images show the homogeneous nature of the few μm thick xerogel films deposited on glass also on the submicron scale, along with the concomitant presence of flower-like Bi_2WO_6 crystallites (Fig. 2).

The successful encapsulation of the flower-like Bi_2WO_6 microparticles in the xerogel matrix was clearly shown by the FSE-SEM analysis at large magnification (×23,000) coupled to the EDS spectra (Fig. 3). The elemental composition of the microparticle returned by electron diffraction confirms the presence of Bi, W, O, Si and C typical of the ORMOSIL-entrapped bismuth wolframate xerogel, whereas film regions

free of dopant species were also clearly detected by the FSE-SEM and EDS analyses (Figs. 2 and 3).

Beyond the results of the FSE-SEM investigation, evidence of successful sol-gel entrapment of bismuth wolframate crystallites in the ORMOSIL matrix was obtained by FT-IR analysis of the powders using an Alpha (Bruker, Billerica, MA, USA) spectrometer equipped with an ATR (attenuated total reflection) ZnSe crystal cell on which the analyte sample is placed. The IR spectra were recorded in the $4000\ cm^{-1}$–$500\ cm^{-1}$ range at resolution of $4\ cm^{-1}$ of THA8 and THA8B in film form and flower-like Bi_2WO_6 in powder form. Fig. 4 clearly unveils the typical dominant band of silica through the signal at $1080\ cm^{-1}$ assigned to the in-phase motion of adjacent oxygen atoms along a line parallel to the Si—Si direction, perpendicularly to the bisector plane, accompanied by the anti-symmetric motion of adjacent Si atoms (ν_{as}Si-O-Si) in both THA8 and THA8B films [18]. Evidence of the successful encapsulation of the perovskite crystallites in the doped film (blue line) is shown by the fingerprint signals of Bi_2WO_6 in the 500–800 cm^{-1} region, with the signals at about 775 and 802 cm^{-1} attributed to the O-W-O bond stretching modes [19].

Evidence of excellent adhesion of both THA8 and THA8B xerogel films on the steel substrates was obtained by characterization of the coatings in terms of adhesion strength, thickness, and contact angle (Table 1).
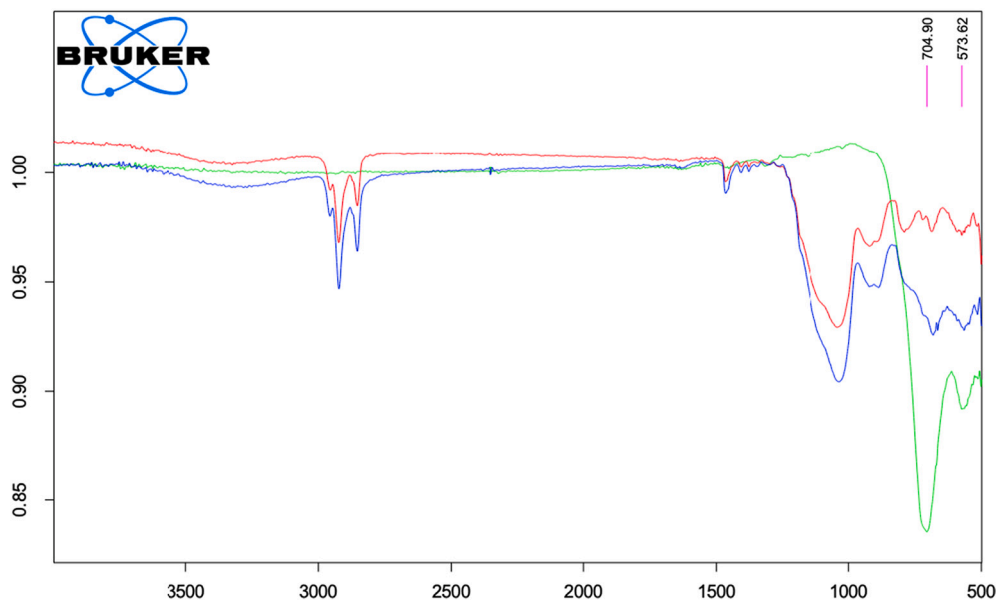
Fig. 4. IR spectra of THA8 (blue line), blank organosilica (red line) and Bi_2WO_6 (green line). (For interpretation of the references to color in this figure legend, the reader is referred to the web version of this article.)

Table 1
Thickness (T), roughness (R_a), Wenzel (θ_w) and Young (θ_Y) contact angles of coatings on steel substrates.

Substrate[a]	T (μm)	R_a (μm)	θ_w (°)	θ_Y (°/μm)
Steel P + T	568	6.76 ± 0.26	81.77 ± 1.76	88.78 ± 1.76
Steel P + T+ THA8	216	2.13 ± 0.04	94.10 ± 1.13	91.92 ± 1.13
Steel P + T+ THA8B	113	9.31 ± 0.25	95.56 ± 1.18	90.59 ± 1.18

[a] P = primer; T = tie coat.

The chromatic map in Fig. 5 indicates a coating thickness of about 200 (216) μm and 100 (113) μm for the THA8 and THA8B coatings, respectively. Precise values along with the thickness of the primer + tie coat coating are given in Table 1.

Data in Table 1 and Fig. 6 show that the corrosion-protected steel substrate with both THA8 and THA8B organosilica coatings impart high contact angle values, confirming the ability of these ORMOSIL-based coatings to impart high hydrophobicity to the coated surface [20]. Fig. 6 shows that the Wenzel and Young contact angle values of the commercial tie-coat, significantly increase after deposition of the THA8 "AquaSun" and THA8B blank ORMOSIL topcoats (p < 0.0001). The presence of the entrapped Bi_2WO_6 in the THA8 coating results in a slightly lower Wenzel angle, but slightly larger Young angle when compared to the blank topcoat.

The cross-cut adhesion test gives a visual comparison method of testing coating adhesion integrity assessed against ISO 2409 and ASTM D 3359 standards, returned the maximum adhesion values for both
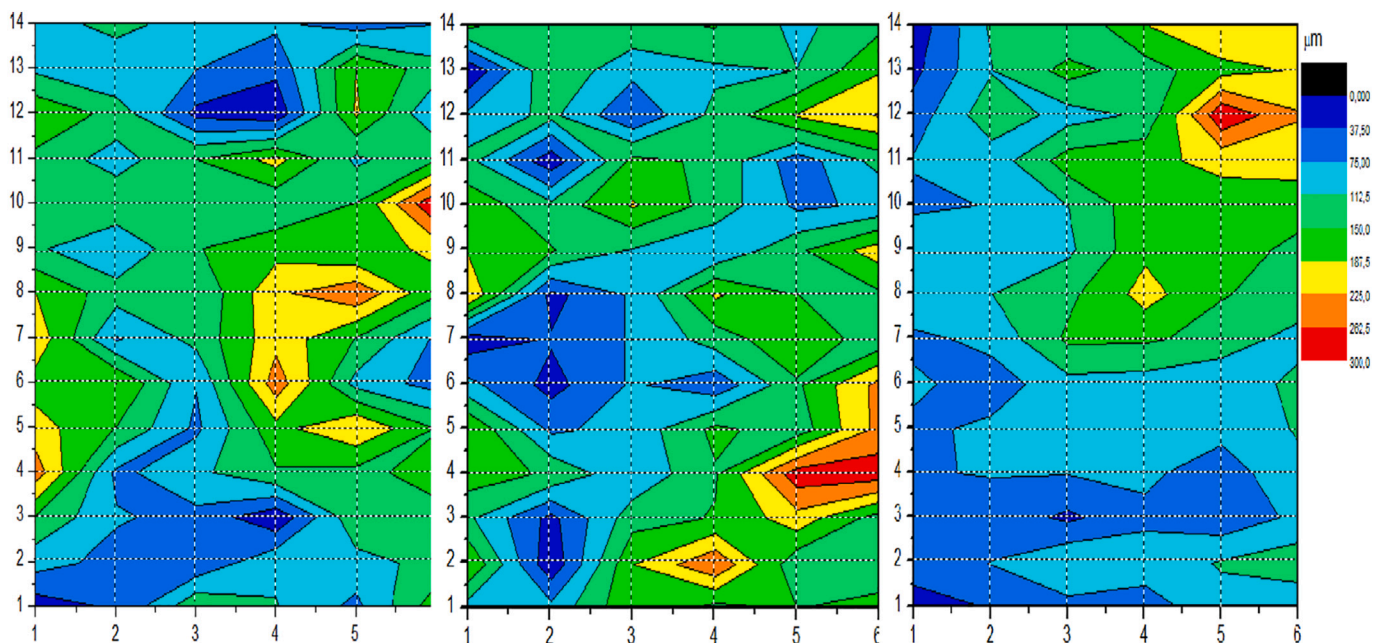

Fig. 5. Chromatic map with the grid 14 × 6 of the metallic specimen in DH36 steel coated with primer (P) + tie coat (T) (left); P + T + THA8 (middle) and P + T + THA8B (right).
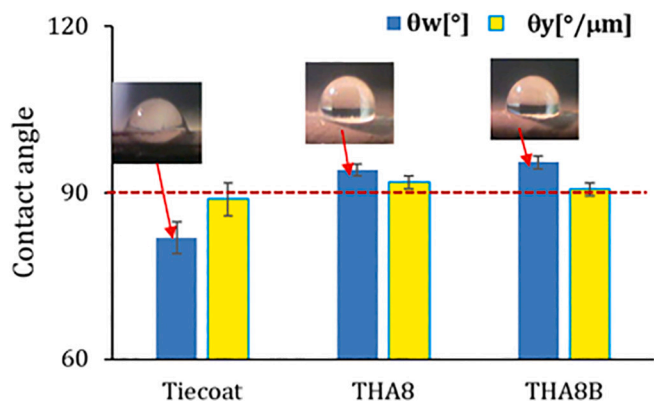
Fig. 6. Wenzel and Young contact angle values of commercial tie coat, and of THA8 and THA8B topcoats on steel substrate.

Fig. 7. Adhesion-cross cut test of commercial tie coat, THA8 and THA8B topcoats.

Table 2
Ecotoxicity tests of AquaSun coatings with *Vibrio fischeri* (MicroTOX test).

Material	EC$_{50}$ mg/L (15 min)	EC$_{50}$ mg/L (30 min)	% Effect 100 mg/L sample (15 min)	% Effect 100 mg/L sample (30 min)
THA6	NL[a]	NL	NL	–
THA6B	NL	NL	NL	–
THA5	NL	NL	NL	–
THA5B	NL	NL	NL	–

[a] NL = within law limits.

substrates, namely ISO 0 and ASTM 5B. We briefly remind that a coating is assigned the ASTM 5B value when the edges of the cuts are completely smooth and none of the squares of the lattice formed upon the cuts is detached [21].

From the utilization viewpoint, as put it by Valli discussing thin hard coatings to protect steel, adhesion is the most important property of a coating [22].
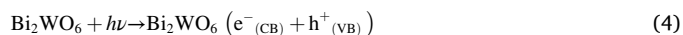
The edges of the cuts shown in Fig. 7 are completely flat, none of the squares of the lattice are detached, in accordance with the reference standards. This uniquely high scratch resistance proves the excellent adhesion levels of these coatings previously obtainable only with physical vapor deposition and chemical vapor deposition techniques [22].

To investigate the ecotoxicity of the AquaSun xerogel films obtained from TEOS and MTES according to the original material preparation route, we carried out the first acute toxicity tests with *Vibrio fischeri* (an *in vitro* test using the bioluminescent bacteria *Aliivibrio fischeri* to detect toxic substances in different environments) according to the published procedure for carrying out the Microtox test [23]. Results in Table 2 show evidence of the complete absence of ecotoxicity.

Further biological tests on the growth of different marine bacteria (*Pseudoaltermonas*, *Alteromonas* and *Pseudomonas*) in the presence of doped and non-doped (blank) AquaSun methylated xerogel films (not shown) fully confirmed that the antifouling activity is due to the photocatalytic action of the AquaSun coatings driven by solar light. Growth of bacteria in the films functionalized with flower-like Bi$_2$WO$_6$ was inhibited by the solar light such as that present in the laboratory where the experiments were conducted.

Inhibition of bacterial population development was especially observed for the 50% methyl-modified film THA 6 whose composition is the same of the optimal AquaSun xerogel coating in our original study, whereas this was not the case for the non-doped (blank) xerogel coatings. We remind here that the photocatalytic reaction on the submarine surface is triggered by visible-light radiation which easily penetrates sea water, with reflection at moderate depths accounting to only 5–10%, while absorption is negligible [24].

When the film is applied on a surface constantly exposed to solar radiation, it continuously produces H$_2$O$_2$ according to Eqs. (4)–(8), in which VB and CB stand, respectively, for valence and conduction band [12]:

$$Bi_2WO_6 + h\nu \rightarrow Bi_2WO_6 \left(e^-_{(CB)} + h^+_{(VB)} \right) \tag{4}$$

$$OH^- + h^+_{(VB)} \rightarrow \dot{O}H \tag{5}$$

$$O_2 + e^-_{(CB)} \rightarrow O_2 - \cdot \tag{6}$$

$$O_2 - \cdot + H^+ \rightarrow HO_2^{\cdot} \tag{7}$$

Table 3
Roughness (R$_a$), Wenzel (θ_w) and Young (θ_Y) contact angles for AquaSun xerogel films deposited on glass substrates.

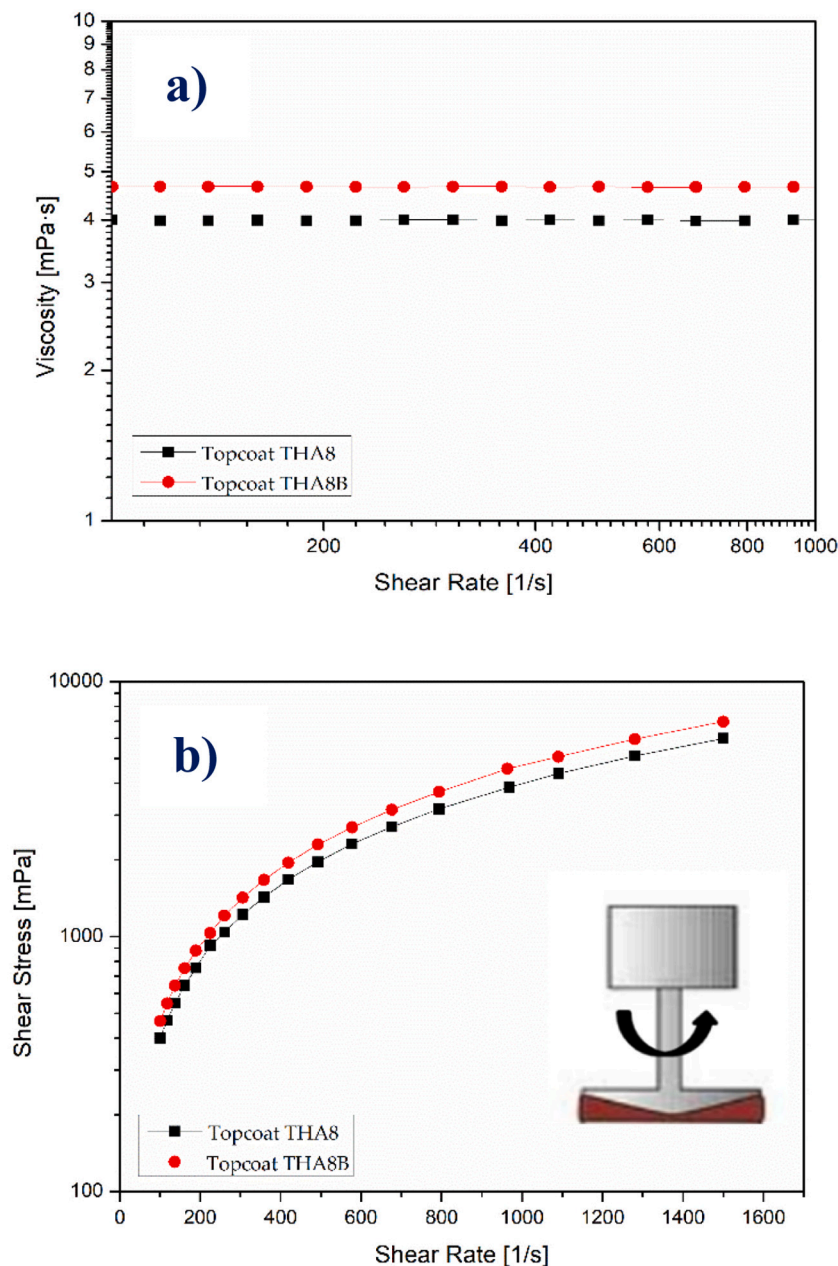| Material	Organic group	DF[a] (%)	Bi$_2$WO$_6$ (mM)	R_a [μm]	θ_w [°]	θ_Y [°/μm]
THA5B	-CH$_3$	10	–	0.053 ± 0.024	95.48 ± 3.07	146.77 ± 3.07
THA5	-CH$_3$	10	50	0.146 ± 0.052	92.54 ± 2.17	130.82 ± 2.17
THA6B	-CH$_3$	50	–	0.558 ± 0.008	91.35 ± 2.51	95.48 ± 2.51
THA6	-CH$_3$	50	50	0.032 ± 0.016	93.05 ± 2.24	137.03 ± 2.24
THA7B	-C$_3$H$_5$	50	–	0.941 ± 0.049	99.31 ± 2.96	97.94 ± 2.96
THA7	-C$_3$H$_5$	50	50	0.17 ± 0.013	97.47 ± 3.95	162.11 ± 3.95
THA8B	-C$_8$H$_{17}$ + -C$_{18}$H$_{37}$	50	–	0.050 ± 0.005	115.57 ± 2.11	168.80 ± 2.11
THA8	-C$_8$H$_{17}$ + -C$_{18}$H$_{37}$	50	50	0.504 ± 0.043	115.39 ± 2.52	148.29 ± 2.52
THA9B	-C$_3$H$_5$ + -C$_{18}$H$_{37}$	50	–	0.012 ± 0.002	101.79 ± 1.98	166.65 ± 1.98
THA9	-C$_3$H$_5$ + -C$_{18}$H$_{37}$	50	50	0.505 ± 0.035	98.19 ± 2.78	106.40 ± 2.78
THA10B	-C$_3$H$_6$-NH$_2$ + -C$_2$H$_2$-CF$_3$	100	–	0.090 ± 0.001	95.44 ± 2.39	170.94 ± 2.39
THA10	-C$_3$H$_6$-NH$_2$ + -C$_2$H$_2$-CF$_3$	100	20	0.081 ± 0.007	93.86 ± 1.57	146.21 ± 1.57

[a] DF = Degree of functionalization.

Fig. 8. Viscosity (a) and flow (b) curves for THA8 and THA8B top coats (inset: cone-plate geometry of the rotational rheometer).

$$2\,HO_2 \xrightarrow{} O_2 + H_2O_2 \tag{8}$$

The ability of ORMOSIL sol-gel coatings to modify the contact angle and the roughness of the coated surface was proven in a broad interval of ORMOSIL xerogel film compositions, using three different alkyl-modified Si alkoxides of different alkyl length (C1, C3, and C18). Results in Table 3 indeed show that the xerogel films obtained with a small amount (1 mol%) of C8 alkyl groups have large surface roughness (THA8B), but that said enhanced roughness is lost when encapsulating the photoactive species Bi_2WO_6 (THA8). The contact angle, however, remains nearly unvaried at 115° namely typical of hydrophobic films (>115°). All groups of contact angle measures are statistically very significant (p < 0.0001).

The roughness values of the coatings (listed in Table 3) are very low, in the range 0.05–0.94 μm, typical of the glass surface on which the film are deposited. Consequently, the coatings are not affected by the roughness of the substrate. Accordingly, the contact angle values are very high, in the super-hydrophobicity range (θ_Y values grow up to

168°). Instead, when the xerogel is deposited on a metallic substrate (such as the DH36 steel coated with primer and tie-coat), the roughness increases reaching up to 9.31 μm (see Table 1), an order of magnitude higher. This increase in the roughness of the substrate causes the Young's contact angle value to decrease to about 92° (hydrophobicity). In general, the values of θ_Y are higher in samples containing the dopant (bismuth wolframate) than in corresponding samples without the dopant species. In particular, the THA10B and THA8B samples are those with super-hydrophobicity values around 170° (168.80° and 170.94°, respectively p < 0.001) on glass substrates.

Fig. 8 shows evidence that the viscosity of the samples remained constant across the entire measuring range of shear rate (0.01–1000 s^{-1}), in agreement to ideally viscous flow behavior. Within the whole shear rate range investigated, the topcoats THA8 and THA8B displayed ideally viscous flow behavior, returning viscosity values of 4 mPas and 4.7 mPas, respectively. In brief, the addition of bismuth wolframate to the xerogel formulation improves the viscosity of the

coating but it does not affect the viscous flow behavior. Coupled to the fact that the workability of the coating does not appreciably change, this is important in sight of forthcoming practical applications of the AquaSun coatings.

4. Conclusions

On path to demonstrate the practical applicability of the new anti-fouling/foul release AquaSun marine sol-gel coating, we report the outcomes of adhesion and ecotoxicity tests carried out on steel specimens faithfully representing the metal surface of real ships, including the topcoat layer typically applied on the ship hull prior to deposition of the antifouling paint. The results of Microtox tests on the first generation AquaSun sol-gel derived organosilica coatings clearly show that Aqua-Sun is an environmentally benign and ecologically safe coating. To enhance the contact angle and make the coating hydrophobic (contact angle >115°), it is enough to replace MTES in the original MTES:TEOS 1:1 composition with a C8:C18 49:1 alkylsilane mixture in full agreement with their early studies on sol-gel organosilica antifouling coatings based on the foul release mechanism [9,17]. The addition of bismuth wolframate does not appreciably alter the coating workability. Preliminary investigation of marine bacteria growth on the coated films confirms previous findings [12,15] that the AF mechanism is indeed due to photocatalysis promoted by the encapsulated Bi_2WO_6.

The key outcome of this investigation, most promising in light of forthcoming practical applications of this new class of antifouling paint, is that these coatings share exceptionally high scratch resistance due to the excellent adhesion of the partly hydrolysed Si alkoxides levels to the hydroxyl groups at the surface of the epoxy-protected steel. Similar maximum values of adhesion strength (ASTM 5B) are observed only for the most resistant coatings usually deposited with expensive physical vapor deposition and chemical vapor deposition techniques [22]. In the context of ongoing research on epoxy-, silane-, and polyurethane-based AF/FR coatings [25], a forthcoming techno-economic study will investigate whether this new class of organosilica-based photocatalytic coatings, merging the foul release properties of sol-gel foul release coatings [11] and the powerful visible-light photocatalytic activity of Bi_2WO_6 [26], is suitable for industrial production.

Data availability

All data reported in this study are freely available by contacting the corresponding Authors.

CRediT authorship contribution statement

Rosaria Ciriminna, Mario Pagliaro, Annamaria Visco: Conceptualization, Methodology; Antonino Scurria, Cristina Scolaro, Silvia Sfameni, Gabriella Di Carlo: Visualization, Investigation; Rosaria Ciriminna, Annamaria Visco: Supervision; Mario Pagliaro: Writing- Original draft preparation; Rosaria Ciriminna, Annamaria Visco: Writing- Reviewing and Editing.

Declaration of competing interest

The authors declare no competing interests.

Acknowledgments

This study is dedicated to the memory of Professor Michael R. Detty (1951-2020). This research was funded by NAVTEC (Consorzio di Ricerca per l'Innovazione tecnologica, Sicilia, Trasporti navali,

commerciali e da diporto s.c.a.r.l), project "Thalassa -TecHnology and materials for safe Low consumption and low life cycle cost veSSels and crafts", grant number ARS01_00293 PON2014-2020. We thank Dr. Simone Cappello, Istituto per le Risorse Biologiche e le Biotecnologie, CNR, for the Microtox eco-toxicological assay measurements.

References

[1] M.P. Schultz, J.A. Bendick, E.R. Holm, W.M. Hertel, Economic impact of biofouling on a naval surface ship, Biofouling 27 (2010) 87–98, https://doi.org/10.1080/08927014.2010.542809.
[2] D. Howell, B. Berhends, Consequences of antifouling coatings - the chemist's perspective in Biofouling, in: S. Dürr, J.C. Thomason (Eds.), Blackwell Publishing, Oxford, 2009, pp. 226–242, https://doi.org/10.1002/9781444315462.ch16.
[3] D. Williams, Challenges in Developing Antifouling Coatings, IMarEST, London, 2010.
[4] Infiniti Research, Global Antifouling Coatings Market 2021-2025, Bengaluru, India, 2021.
[5] I. Amara, W. Miled, R. Ben Slama, N. Ladhari, Antifouling processes and toxicity effects of antifouling paints on marine environment. A review, Environ. Toxicol. Pharmacol. 57 (2018) 115–130, https://doi.org/10.1016/j.etap.2017.12.001.
[6] F. Cima, R. Varello, Potential disruptive effects of copper-based antifouling paints on the biodiversity of coastal macrofouling communities, Research Square (2021), https://doi.org/10.21203/rs.3.rs-827075/v1.
[7] R. Ciriminna, F.V. Bright, M. Pagliaro, Ecofriendly antifouling marine coatings, ACS Sustain. Chem. Eng. 3 (2015) 559–565, https://doi.org/10.1021/sc500845n.
[8] S.K. Kyei, G. Darko, O. Akaranta, Chemistry and application of emerging ecofriendly antifouling paints: a review, J. Coat. Technol. Res. 17 (2020) 315–332, https://doi.org/10.1007/s11998-019-00294-3.
[9] Y. Tang, J.A. Finlay, G.L. Kowalke, A.E. Meyer, F.V. Bright, M.E. Callow, J. A. Callow, D.E. Wendt, M.R. Detty, Hybrid xerogel films as novel coatings for antifouling and fouling release, Biofouling 21 (2005) 59–71, https://doi.org/10.1080/08927010500070935.
[10] M.R. Detty, R. Ciriminna, F.V. Bright, M. Pagliaro, Xerogel coatings produced by the sol–gel process as anti-fouling, fouling-release surfaces: from lab bench to commercial reality, ChemNanoMat 1 (2015) 148–154, https://doi.org/10.1002/cnma.201500056.
[11] M.R. Detty, R. Ciriminna, F.V. Bright, M. Pagliaro, Environmentally benign sol–gel antifouling and foul-releasing coatings, Acc. Chem. Res. 47 (2014) 678–687, https://doi.org/10.1021/ar400240n.
[12] G. Scandura, R. Ciriminna, Y.-J. Xu, M. Pagliaro, G. Palmisano, Nanoflower-like Bi2WO6 encapsulated in ORMOSIL as a novel photocatalytic antifouling and foul-release coating, Chem. Eur. J. 22 (2016) 7063–7067, https://doi.org/10.1002/chem.201600831.
[13] S.M. Olsen, J.B. Kristensen, B.S. Laursen, L.T. Pedersen, K. Dam-Johansen, S. Kiil, Antifouling effect of hydrogen peroxide release from enzymatic marine coatings: exposure testing under equatorial and Mediterranean conditions, Prog. Org. Coat. 68 (2010) 248–252, https://doi.org/10.1016/j.porgcoat.2010.01.003.
[14] H. Elzanowska, R.G. Wolcott, D.M. Hannum, J.K. Hurst, Bactericidal properties of hydrogen peroxide and copper or iron-containing complex ions in relation to leukocyte function, Free Radic. Biol. Med. 18 (1995) 437–449, https://doi.org/10.1016/0891-5849(94)00150-I.
[15] G. Scandura, R. Ciriminna, L. Yıldız Ozer, F. Meneguzzo, G. Palmisano, M. Pagliaro, Antifouling and photocatalytic antibacterial activity of the AquaSun coating in seawater and related media, ACS Omega 2 (2017) 7568–7575, https://doi.org/10.1021/acsomega.7b01237.
[16] P.G. Falkowski, The role of phytoplankton photosynthesis in global biogeochemical cycles, Photosynth. Res. 39 (1994) 235–258, https://doi.org/10.1007/BF00014586.
[17] N. Gunari, L.H. Brewer, S.M. Bennett, A. Sokolova, N.D. Kraut, J.A. Finlay, A. E. Meyer, G.C. Walker, D.E. Wendt, M.E. Callow, J.A. Callow, F.V. Bright, M. R. Detty, The control of marine biofouling on xerogel surfaces with nanometer-scale topography, Biofouling 27 (2011) 137–149, https://doi.org/10.1080/08927014.2010.548599.
[18] A. Fidalgo, L.M. Ilharco, Chemical tailoring of porous silica xerogels: local structure by vibrational spectroscopy, Chem. Eur. J. 10 (2004) 392–398, https://doi.org/10.1002/chem.200305079.
[19] G. Li, Electrospinning fabrication and photocatalytic activity of Bi2WO6 nanofibers, J. Mater. Sci. Mater. Electron. 28 (2017) 12320–12325, https://doi.org/10.1007/s10854-017-7050-z.
[20] M. Pagliaro, R. Ciriminna, G. Palmisano, Silica-based hybrid coatings, J. Mater. Chem. 19 (2009) 3116–3126, https://doi.org/10.1039/b819615j.
[21] ASTM D 3359–92a, Standard Test Methods for Measuring Adhesion by Tape Test, ASTM, 1992.
[22] J. Valli, A review of adhesion test methods for thin hard coatings, J. Vac. Sci. Technol. A 4 (1986) 3007–3012, https://doi.org/10.1116/1.573616.
[23] B.T. Johnson, Microtox acute toxicity test, in: C. Blaise, J.F. Férard (Eds.), Small-scale Freshwater Toxicity Investigations, Springer, Dordrecht, 2005, https://doi.org/10.1007/1-4020-3120-3_2.

[24] D.M. McMaster, S.M. Bennett, Y. Tang, J.A. Finlay, G.L. Kowalke, B. Nedved, F. V. Bright, M.E. Callow, J.A. Callow, D.E. Wendt, M.G. Hadfield, M.R. Detty, Antifouling character of 'active' hybrid xerogel coatings with sequestered catalysts for the activation of hydrogen peroxide, Biofouling 25 (2009) 21–33, https://doi.org/10.1080/08927010802431298.

[25] A. Pistone, C. Scolaro, A. Visco, Mechanical properties of protective coatings against marine fouling: a review, Polymers 13 (2021) 173, https://doi.org/10.3390/polym13020173.

[26] N. Zhang, R. Ciriminna, M. Pagliaro, Y.-J. Xu, Nanochemistry-derived Bi2WO6 nanostructures: towards sustainable chemicals and fuels production induced by visible light, Chem. Soc. Rev. 43 (2014) 5276–5287, https://doi.org/10.1039/c4cs00056k.